AL/CF-TR-1996-0121

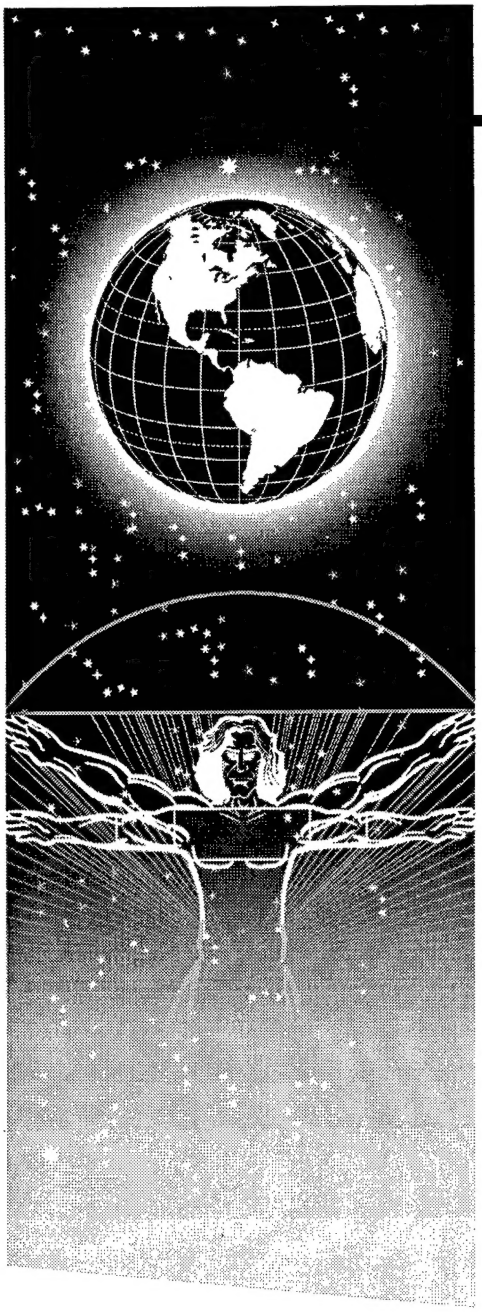

UNITED STATES AIR FORCE
ARMSTRONG LABORATORY

HUMAN PERFORMANCE AIDING FOR TACTICAL DECISION AIDS AND MISSION PERFORMANCE AIDS: A MODEL OF HUMAN VISUAL PERFORMANCE FOR THE WEATHER IMPACT DECISION AID (WIDA) ELECTRO-OPTICAL SIMULATION (ACT/EOS)

Gregg E. Irvin

SCIENCE APPLICATIONS INTERNATIONAL CORP.
1321 RESEARCH PARK DRIVE
DAYTON OH 45432

Denise L. Aleva

CREW SYSTEMS DIRECTORATE
HUMAN ENGINEERING DIVISION
WRIGHT-PATTERSON AFB OH 45433-7022

James P. Gaska
Lowell D. Jacobson

UNIVERSITY OF MASSACHUSETTS
MEDICAL SCHOOL
WORCESTER MA

MARCH 1996

FINAL REPORT FOR THE PERIOD SEPTEMBER 1992 TO MARCH 1994

Crew Systems Directorate
Human Engineering Division
2255 H Street
Wright-Patterson AFB, OH 45433-7022

NOTICES

When US Government drawings, specifications, or other data are used for any purpose other than a definitely related Government procurement operation, the Government thereby incurs no responsibility nor any obligation whatsoever, and the fact that the Government may have formulated, furnished, or in any way supplied the said drawings, specifications, or other data, is not to be regarded by implication or otherwise, as in any manner licensing the holder or any other person or corporation, or conveying any rights or permission to manufacture, use, or sell any patented invention that may in any way be related thereto.

Please do not request copies of this report from the Armstrong Laboratory. Additional copies may be purchased from:

National Technical Information Service
5285 Port Royal Road
Springfield, Virginia 22161

Federal Government agencies and their contractors registered with the Defense Technical Information Center should direct requests for copies of this report to:

Defense Technical Information Center
8725 John J. Kingman Road, Suite 0944
Ft. Belvoir, Virginia 22060-6218

TECHNICAL REVIEW AND APPROVAL

AL/CF-TR-1996-0121

This report has been reviewed by the Office of Public Affairs (PA) and is releasable to the National Technical Information Service (NTIS). At NTIS, it will be available to the general public, including foreign nations.

This technical report has been reviewed and is approved for publication.

FOR THE COMMANDER

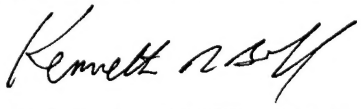

KENNETH R. BOFF, Chief
Human Engineering Division
Armstrong Laboratory

REPORT DOCUMENTATION PAGE

Form Approved
OMB No. 0704-0188

1. AGENCY USE ONLY (Leave blank)	2. REPORT DATE	3. REPORT TYPE AND DATES COVERED
	March 1996	FINAL (September 1992-March 1994)

4. TITLE AND SUBTITLE Human Performance Aiding for Tactical Decision Decision Aids and Mission Performance Aids: A Model of Human Visual Performance for the Weather Impact Decision Aid (WIDA) Electro-Optical Simulation (ACT/EOS)

5. FUNDING NUMBERS
PE 63070F
PR 6893
TA 01
WU 35

6. AUTHOR(S)

Gregg E. Irvin* Denise L. Aleva
James P. Gaska** Lowell D. Jacobson**

7. PERFORMING ORGANIZATION NAME(S) AND ADDRESS(ES)

* Science Applications International Corporation
1321 Research Park Drive
Dayton OH 45432

8. PERFORMING ORGANIZATION REPORT NUMBER

9. SPONSORING/MONITORING AGENCY NAME(S) AND ADDRESS(ES)
Armstrong Laboratory, Crew Systems Directorate
Human Engineering Division
Human Systems Center
Air Force Materiel Command
Wright-Patterson AFB OH 45433-7022

10. SPONSORING/MONITORING AGENCY REPORT NUMBER
AL/CF-TR-1996-0121

11. SUPPLEMENTARY NOTES
** University of Massachusetts
Medical School
Worcester MA

12a. DISTRIBUTION/AVAILABILITY STATEMENT
Approved for public release; distribution is unlimited

12b. DISTRIBUTION CODE

13. ABSTRACT *(Maximum 200 words)*

The Human Performance Model (HPM) was developed as part of the Infrared Tactical Decision Aid Human Performance Modeling and Analysis Program. The Infrared Tactical Decision Aid (IRTDA) was developed by Air Weather Service as an analysis tool that helps a commander decide how to deploy forces and weapons by providing accurate range predictions of a pilot's ability to detect, identify, and recognize a target given a particular set of weather conditions and a particular sensor. The objective of the IRTDA development program was the accurate prediction of human performance using IR weapons systems. The modeling includes target/background scene (Thermal Contrast Model, TCM2), target/sensor transmission (Atmospheric Transmission Model LOTRAN7), and, both sensor and human performance (Sensor Performance Model, SPM). TCM2, LOTRAN7, and the sensor portion of the SPM are refined computational models, approaching essentially, first principle models. However, the human portion of the SPM is theoretically inadequate and produces 'order of magnitude' predictive error. The current effort solves this problem and provides broader predictive capability. This is accomplished by multiscale space/spatial frequency modeling and applying perceptually based algorithms to establish new criteria for detection, identification, and recognition ranges.

14. SUBJECT TERMS
Tactical Decision Aid, human modeling, human performance perception, visual modeling, space/spatial frequency, detection identification, recognition, luminance gain, contrast gain

15. NUMBER OF PAGES
29

16. PRICE CODE

17. SECURITY CLASSIFICATION OF REPORT	18. SECURITY CLASSIFICATION OF THIS PAGE	19. SECURITY CLASSIFICATION OF ABSTRACT	20. LIMITATION OF ABSTRACT
Unclassified	Unclassified	Unclassified	Unlimited

This Page Intentionally Left Blank

Table of Contents

Table of Figures

1. INTRODUCTION

1.1 General Overview of the Human Performance Modeling Effort

The Human Performance Model (HPM) was developed as a part of the Infrared Tactical Decision Aid Human Performance Modeling and Analysis Program. The HPM effort describes an approach for the modification of the sensor performance model component of Tactical Decision Aids (TDA) to enable the accurate prediction of human visual detection, identification and recognition ranging algorithms for various target classes. Additionally, the HPM greatly broadens predictive capability to any arbitrary target or target complex, and to any background clutter conditions.

An observer model is incorporated which more completely utilizes information in the detailed thermal image generated by the advanced Thermal Contrast Model (TCM2). The general approach involves taking the present sensor performance model and subdividing it into independent sensor, display, and observer models. The sensor model receives as input the atmospherically transformed 2D target/background image produced by TCM2 and produces a 2D image output that reflects the sensor transformation/degradation only. The display model receives as input the sensor output image and similarly applies the display transformation/degradation to simulate the actual visual stimulus (cockpit display) seen by a human pilot.

The HPM transforms the output of the display module (i.e. the predicted cockpit display image) into a space/spatial frequency (S/SF) representation. This representation is a multiple spatial frequency channel pyramid representation that simulates the encoding used by the human visual system. The representation takes the form of a 4-D space/spatial frequency transform using gabor basis filters, known as the Hexagonal Orthogonal Oriented Pyramid. The image processing transformations represent modern vision theory and are based on current psychophysical and neurophysiological experimentation and models. The representation incorporates both luminance gain control (LGC) and contrast gain control (CGC) algorithms. The LGC models the changes in spatiotemporal contrast sensitivity which occur as a function of ambient illumination. The CGC models the changes in sensitivity which occur locally in the visual system due to local contrast distribution variations in a scene allowing the cortical representation for input images with any arbitrary contrast distribution.

Predictions about observer performance are then obtained by applying decision operators in a simulated pairwise discrimination task to the population of mechanisms in the visual encoding representation. The paired comparisons task is amenable to reformulation for the accurate prediction of a wide range of visual performance tasks such as detection, identification and recognition ranges, or, in more complicated tasks such as detecting distributed targets in cluttered backgrounds.

1.2 Background

The Infrared Tactical Decision Aid (IRTDA) was developed by Air Weather Service as an analysis tool that helps a commander decide how to deploy forces and weapons by providing accurate range predictions of a pilot's ability to detect, identify, and recognize a target given a particular set of weather conditions and a particular sensor. The objective of the IRTDA development program was the accurate prediction of the performance of the IR weapons system including both precision guided munitions (e.g. I^2R Maverick) and on-board aircraft target acquisition systems (e.g. LANTIRN). The existing IRTDA consists of three main components: a) the Thermal Contrast Model (TCM2) predicts the target/background scene, b) the Atmospheric Transmission Model (LOTRAN7) models the transmission from the target to the sensor, and c) the Sensor Performance Model (SPM) then predicts sensor performance and the maximal detection, identification, and recognition (DIR) ranges of the human observer.

Over the years, both the TCM2 and LOTRAN7 have evolved into refined computational approaches founded in verified fundamental physical principles and essentially approach first principle models. As such, they have served as successful engineering models with broad application to problems involving infrared (IR) image prediction. The SPM lumps together both the sensor modeling and observer modeling. The sensor portion of the SPM has also been very successful in its predictive abilities. However, the observer portion of the SPM can produce 'order of magnitude' predictive error. The SPM has suffered from the same empirical model that was used in the early versions of the system, which is based upon empirical results obtained by John Johnson (Johnson, 1958). Updating the human observer portion of the SPM has failed to keep pace with advances in the other IRTDA model components.

The purpose of the IRTDA Human Performance Modeling and Analysis Program was to correct the current shortcomings and broaden the predictive capability of the IRTDA model to include new high value target classes. The IRTDA Human Performance Modeling and Analysis Program has demonstrated why the current SPM is insufficient to characterize the performance of an observer and provides a solution based on principles which have emerged in human visual science over the last two decades. This effort resulted in the Human Performance Model (HPM). The sections below describe the architecture and major components of the HPM Human Performance Model, the system parameters and calibration, and, the models' applicability.

The HPM offers several advantages including the exploitation of all target facet information from TCM2, and, applicability to a wide range of targets and backgrounds with complex shapes and internal structures. Additionally, the approach is modular and allows for independent model testing.

2. OVERVIEW OF MODEL

2.1 General Description of the Human Performance Model

The Human Performance Model (HPM) is a computational model of human visual discrimination. That is, given a pair of input images, the HPM can predict whether an average human observer can reliably discriminate between those two images.

Figure 1 summarizes the signal flow and major transformation stages in the HPM. First, the HPM receives, as input, a pair of two-dimensional achromatic images, denoted respectively as the *target* and *background* images. Second, each image is transformed into a separate four-dimensional *cortical representation* that serves to approximate the distributed neural image representation found in the primary visual cortex of humans when viewing that same image. Third, a difference vector is formed by subtracting the cortical representation of the background image from the cortical representation of the target image. Finally, the elements in the difference vector are pooled in a nonlinear fashion to obtain a single non-negative sensitivity value.

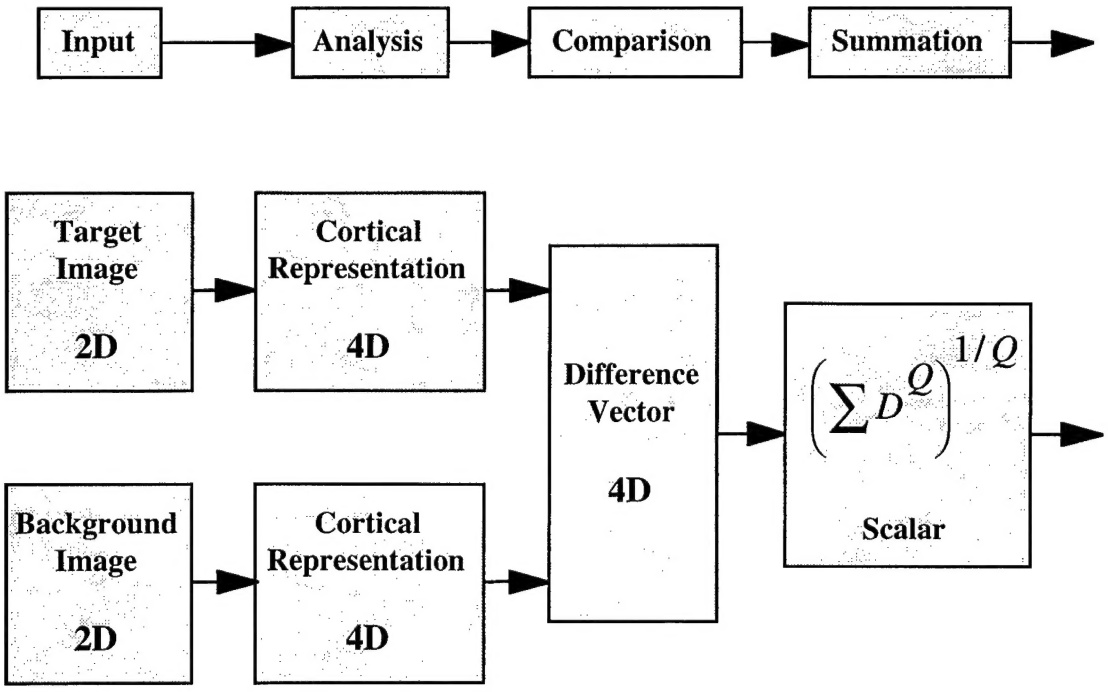

Figure 1. Overview of the Human Performance Model.

The sensitivity value is the sole output of the HPM. By definition, a sensitivity value of 0.0 is obtained from identical images, a value of 1.0 is obtained from images whose small difference places them near the threshold for visual discrimination, and a value much larger than 1.0 is obtained from an image pair that is highly discriminable. As

discussed below, the output of the Human Performance Model (D) can be converted into a predicted probability of correct discrimination.

2.2 Computing a Cortical Representation

As indicated in the analysis stage of Figure 1, the HPM transforms each input image into a four-dimensional *cortical representation.* This cortical representation serves to approximate the distributed neural image representation found in the primary visual cortex of humans when viewing each image. The steps required to compute the cortical representation are depicted in Figure 2 below. The three major transformation stages are the luminance gain control, the space/spatial-frequency transform, and the contrast gain control. These three stages are briefly discussed below.

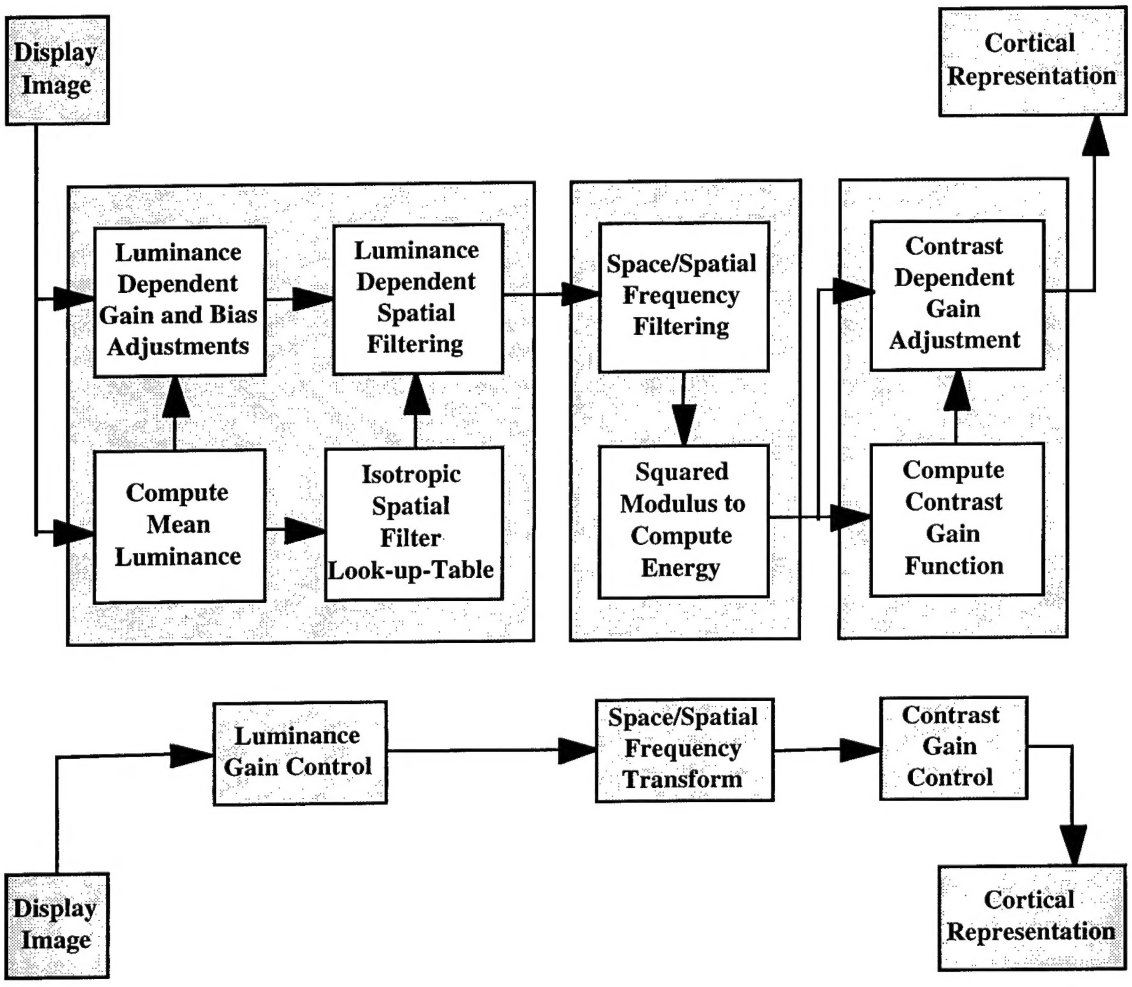

Figure 2. Block Diagram of computing a cortical representation.

2.2.1 Luminance Gain Control

As with all biological neurons, neurons in the early visual system have a very limited dynamic range of approximately 2 orders of magnitude (10^2). Yet these neurons respond in a graded fashion to luminance over a much larger range spanning about 10 orders of magnitude (10^{10}). The early visual system accomplishes this feat by dynamically adjusting its sensitivity in accordance with the prevailing mean luminance of the imaged scene. As a result, the spatial contrast sensitivity of the human visual system varies dramatically as a function of mean luminance. These changes are reflected not only in the scale, but also the shape, of human sensitivity to spatial sinewave gratings (Kelly, 1972). The causes of these luminance-related sensitivity changes are both optical and neural. With regard to optical causes, one must consider the effect of pupillary size adaptation. With regard to neural causes, one must consider the effect of sensitivity changes and spatial filtering by neurons in both the retina and the lateral geniculate nucleus (LGN). The luminance gain control module models the overall effect of the known mechanisms which contribute to these gain changes. As shown in Figure 2, the luminance gain control is implemented as a set of luminance-dependent spatial filters. The shapes and gains of these spatial filters were chosen to model the neurophysiological data from higher primates and the psychophysical data from human subjects.

2.2.2 Space/Spatial Frequency Transform

During the past three decades, psychophysical and neurophysiological experiments have established that, for each subregion in visual space, there is a set of neurons in the primary visual cortex whose members are each selective for a different limited region in 2-D spatial frequency. This discovery precipitated a revolution in computational visual science leading to a new generation of models of visual function in which the cortical representation takes the form of a 4-D space/spatial frequency ***wavelet*** transform (for a review see Watson, 1990). A wavelet transform is one in which the basis functions can all be made equal to a master wavelet by scaling or rotation. The master wavelet in visual cortex models is generally bandpass and oriented, and it is generally complex-valued, having real and imaginary components with a quadrature phase relationship. The HPM uses a transform, known as the Hexagonal Orthogonal Oriented Pyramid (HOP) transform, based on a gabor basis function representation that satisfies the above properties (Watson and Ahumada, 1987). The HOP transform is a complete, orthogonal wavelet transform. During this project, a FAST HOP transform algorithm was developed for use in the HPM. As indicated in Figure 2, after computing the HOP transform, the HPM computes a squared modulus to obtain a space/spatial frequency ***energy*** representation. An energy representation is known to be encoded by the class of cells in the primary visual cortex known as *complex* cells which provide the major input to higher

cortical visual areas in humans. As such, this neuronal class is believed to be critical to visual pattern recognition in humans.

2.2.3 Contrast Gain Control

The human visual system locally adapts its contrast sensitivity in accordance with the local retinal contrast distribution provided in a visual scene. Such contrast adaptation is most evident in psychophysical experiments that involve moderate to high contrast stimuli. Recently, it has been established that neurons in the primary visual cortex typically show a similar adaptation. Such adaptation by cortical neurons is modeled within the HPM by the contrast gain control module illustrated in Figure 2. Details of the adaptation model are described in a later section of this report. The parameters that govern the contrast gain control were chosen to optimize the capability of the HPM to predict published contrast sensitivity data obtained in human psychophysical experiments.

2.3 Multiple Mechanism Detector

2.3.1 Theory

In order to relate the model to human behavior we must first define the visual discrimination task. In what follows we assume that the task is a two-alternative forced choice task in which the observer views two stimuli, a base stimulus and a base + test stimulus, and must report which of the two stimuli contained the test. Under these conditions, the observer's psychometric function (probability of correct discrimination as a function of stimulus contrast) will vary from 0.5 when the observer is simply guessing to 1.0 for perfect discrimination performance. Quick (1974) has shown that human psychometric functions are well described by the following equation:

$$\psi_Q(C) = 1 - 2^{-[1+(SC)^Q]}$$

where C is the contrast of the test stimulus, S is the sensitivity of the visual system to the test stimulus, and Q is a variable that determines the steepness of the psychometric function. For this function the product of SC is equal to unity when the probability of correct detection is 0.75. Therefore, if we define threshold as a 0.75 probability of correct detection, then S is simply the reciprocal of the test contrast at threshold.

Examples of the Quick psychometric function are shown in Figure 3. Note that when test contrast is equal to 1/S then the probability of correct discrimination is 0.75. Comparison of the two curves on the right shows how increasing Q increases the steepness of the psychometric function.

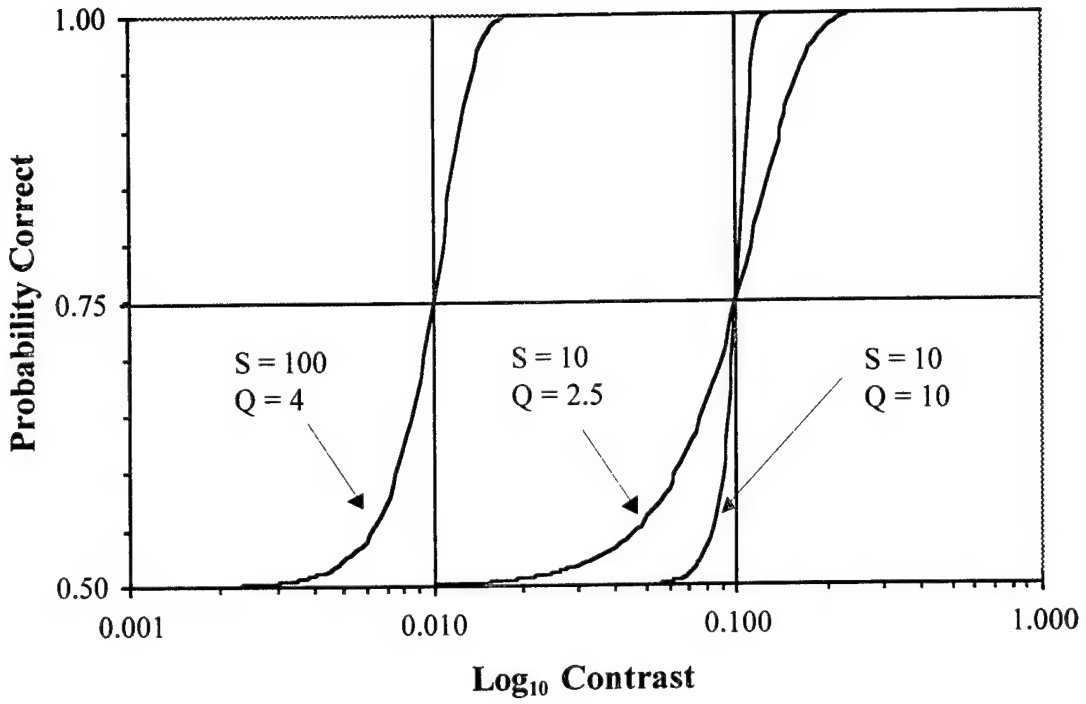

Figure 3. Quick psychometric function for a two-alternative forced choice experiment.

The importance of the Quick formulation is that it provides a simple way to compute the overall sensitivity of a system with multiple mechanisms. Figure 4 shows the human performance model expressed schematically as a multichannel model with noise added prior to signal detection.

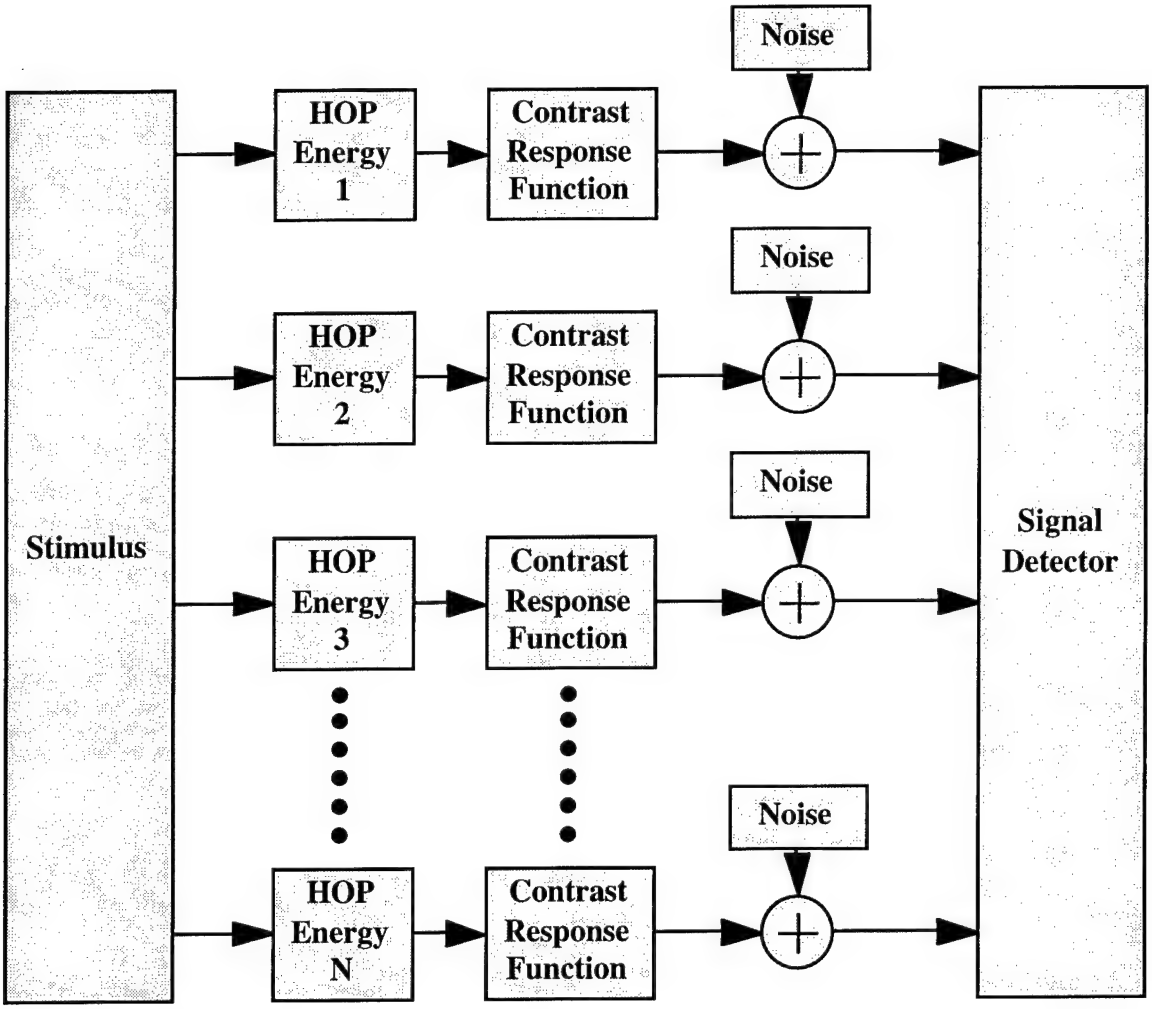

Figure 4. Multiple Mechanism Model with Noise Perturbation.

Quick showed that the overall sensitivity of a multichannel system with individual channel sensitivities S_i is given by the following equation:

$$S = \frac{1}{C_{thresh}} = \left[\sum_i |S_i|^Q \right]^{1/Q}$$

where S is the Human Performance Model sensitivity, C_{thresh} is contrast at threshold , S_i is the sensitivity of the i_{th} channel and the Quick exponent, Q, is the steepness parameter given above. Quick's original formulation was limited to threshold stimuli and did not include a nonlinear contrast response function which is necessary to account for suprathreshold sensitivity. However, Wilson (1980) extended Quick's formulation to suprathreshold systems and showed that the overall sensitivity of the Human Performance Model shown above is given by:

$$S = \frac{1}{C_{thresh}} = \left[\sum_i |S_i|^{PQ} \right]^{1/PQ}$$

This function is exactly the same as Quick's function except that the exponent Q has been replaced by the product PQ where P is the correlation between the noise processes added to each mechanism. Thus PQ will only equal Q when P =1.0, i.e., when the noise among mechanisms is perfectly correlated. There is at present no conclusive evidence concerning the degree to which the noise is correlated among visual channels. Psychophysical experiments can only measure the product PQ which varies from roughly 2.5 - 4.5 for threshold studies and increases when discriminating high contrast stimuli. Because we cannot determine the values of P and Q, we will assume for simplicity that the noise among the detectors is perfectly correlated (PQ = Q). Note that it is the product PQ that is important for predicting the discrimination behavior of human observers. Thus while the noise correlation among channels is important from a theoretical perspective, it will not affect the model's predictions of discrimination thresholds.

3. HUMAN PERFORMANCE MODEL SYSTEM PARAMETERS AND CALIBRATION

The Human Performance Model was calibrated by comparing the output of the model with psychophysical data. A simplex minimization routine (Press, Flannery, Teukolsky and Vetterling, 1988) was used to change the parameters of the model in order to minimize the difference between the output of the model and the psychophysical data. In what follows we first describe the detector that will be used in the model. We then show how the Human Performance Model generates threshold data. Finally we discuss the psychophysical data that was used to calibrate the HPM and show the results of the calibration.

3.1 Computing Discrimination Thresholds

Psychopysical data are often reported using ***threshold contrast*** (the contrast required for detection or discrimination) or ***contrast sensitivity*** (the reciprocal of threshold contrast). Because we wish to use psychophysical data to calibrate the Human Performance Model we must compute HPM System contrast thresholds. The equation used to compute contrast thresholds uses the Quick-Wilson formulation:

$$D(c) = \left[\sum_i |Rtest_i(c) - Rbase_i(c)|^Q \right]^{1/Q}$$

where $Rtest_i(c)$ is the response of the ith cortical mechanism to the test stimulus, $Rbase_i(c)$ is the response of the ith cortical mechanism to the base stimulus, and $D(c)$ is a scalar representing the discriminability of the two stimuli. From the prior discussion it follows that when $D(c)=1$ then C is equal to the discrimination contrast threshold of the HPM and $1/C$ is the discrimination contrast sensitivity of the HPM. To find discrimination contrast thresholds we iteratively changed the contrast of the test stimulus input to the model until $R(c)=1$ (within a 0.01% tolerance). Note, for absolute thresholds (in which an observer is forced to discriminate between a test stimulus and a blank screen), $Rbase_i(c)=0$ for all i so the differencing operation can be omitted.

The model was calibrated by comparing the thresholds of the model to human psychophysical data and adjusting the parameter values until the difference between the model and the data was minimized. The error for a given set of stimuli was computed as

$$error = \sum \left| \ln(\text{Model Threshold}) - \ln(\text{Psycophysical Threshold}) \right|$$

and a simplex minimization routine (Press, Flannery, Teukolsky and Vetterling, 1988) was used to iterate the Human Performance Model parameters until the error was minimized. The natural logarithm of the data was used because the error bars for psychophysical data is approximately normalized when the data is plotted on a logarithmic scale.

3.2 Luminance Gain Control

3.2.1 Psycophysical Data

The curves shown in Figure 5 were generated using an equation developed by Barten (1990). The equation describes the effects of mean luminance and image size on human contrast sensitivity and was developed from experimental data collected by van Meeterin (1973) and Carlson (1982). The Barten equation was used to calibrate the HPM. It has two major benefits. First, the equation describes the dependence of contrast sensitivity functions on both mean luminance and stimulus size. Second, the data were collected under conditions that correspond to those of a pilot in a cockpit, i.e., observation with both eyes, natural pupils and prolonged viewing time.

A given curve in Figure 5 shows how human contrast sensitivity changes with spatial frequency. The top curve represents sensitivities measured at a mean luminance of 1000 candela/meter^2. For each successively lower curve the mean luminance was reduced by an order of magnitude (a factor of 10). The majority of display monitors have mean luminances in the range of 1 to 500 candela/meter^2.

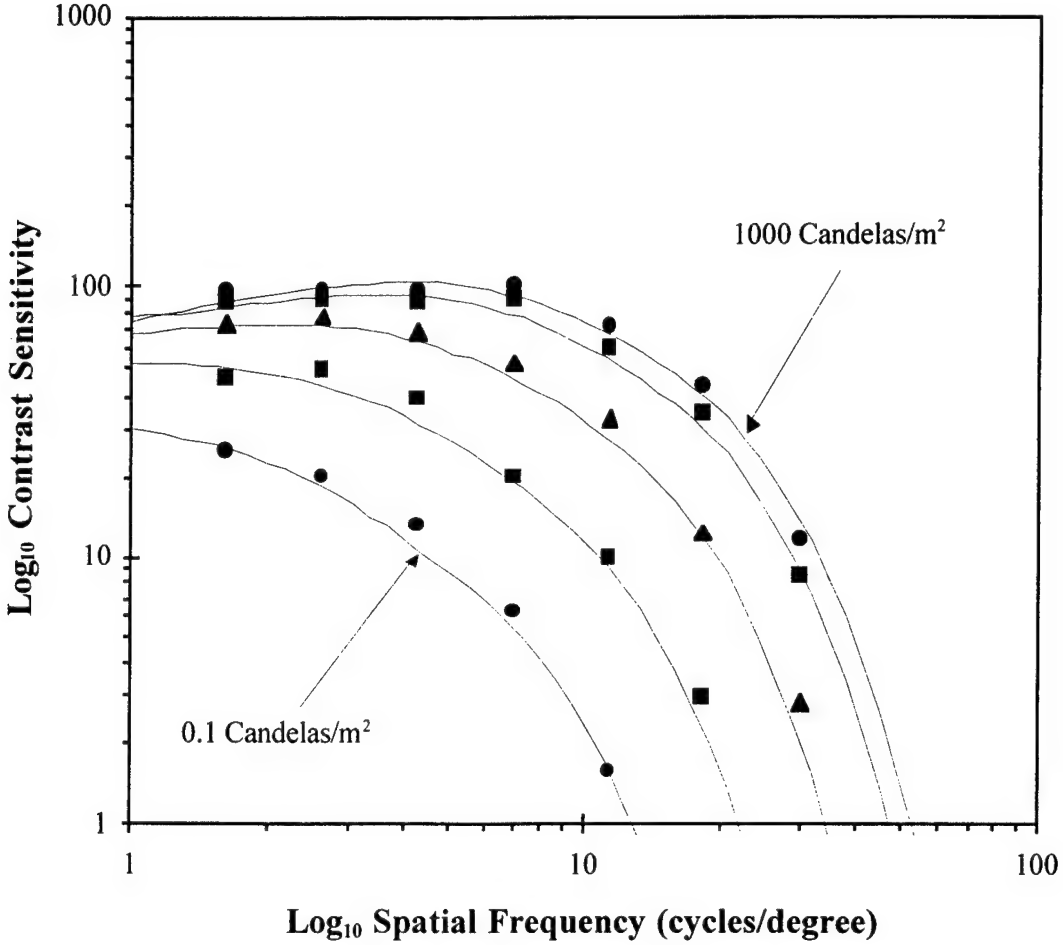

Figure 5. Effects of mean luminance on contrast sensitivity.

Inspection of Figure 5 shows that contrast sensitivity increases with mean luminance. These luminance-dependent gain changes are quite large particularly at high spatial frequencies. For example at 1 cycle/degree sensitivity changes by about a factor of about 2.5 over the full range of mean luminances and at 10 cycles/degree the sensitivities change by about a factor of 25.

Those familiar with contrast sensitivity functions may have noticed the low frequency falloff of the curves in Figure 5 above are much more gradual than those typically presented in vision research literature. This is because contrast sensitivity functions are typically measured using a grating stimulus that has a fixed size. Because the spatial frequency bandwidth of a sinewave grating stimulus is constant for all spatial frequencies when grating size is held constant, we will refer to these more typical measurements as ***constant absolute bandwidth*** contrast sensitivity functions.

The contrast sensitivity functions in Figure 5 result when the width of the sine wave grating changes such that

$$Width(\text{deg}) \times SpatialFrequency(cycles / \text{deg}) = 1.5(cycles).$$

We will refer to these functions as ***constant relative bandwidth*** contrast sensitivity functions because the stimulus spatial frequency bandwidth is constant when measured in octaves. The utility of using constant relative bandwidth stimuli with 1.5 cycles to calibrate the HPM follows from the fact that such stimuli are consistent with neurophysiological data and are similar in shape to the linear filters of the HOP transform. Because of the close match between the stimuli and the HOP filters, a 1.5 cycle grating will only produce robust responses in a few cortical mechanisms and pooling (probability summation) across mechanisms is minimized. Thus, 1.5 cycle constant relative bandwidth contrast sensitivity functions closely approximate the luminance gain control required by the HPM and are particularly useful in calibrating the luminance gain control parameters of the HPM. The symbols in Figure 5 represent the model's fit to the Barten functions which were derived from empirical data.

3.2.2 System Equation

The luminance gain control module was implemented in the model as a luminance-dependent two-dimensional difference of Gaussians (DOG) linear filter. This filter is convolved with the input image and has the effect of attenuating the contrast of the image in a frequency dependent manner. The form of the function is as follows:

$$f(r) = M_{center} \exp^{-\frac{1}{2}\left(\frac{r}{\sigma_{center}}\right)^2} - M_{surround} \exp^{-\frac{1}{2}\left(\frac{r}{\sigma_{surround}}\right)^2}$$

where r is the radial distance (in degrees of visual angle), and M_{center}, $M_{surround}$, σ_{center} and $\sigma_{surround}$ are parameters to be fit as a function of luminance. The function is a very good fit to the spatial weighting function of neurons in the retina (Rodiack, 1965) and lateral geniculate nucleus (Irvin, Casagrande and Norton, 1993; Irvin, Norton and Casagrande, 1986).

3.3 Probability Summation Across Mechanisms

3.3.1 Psychophysical Data

Figure 6 compares a constant relative bandwidth contrast sensitivity function (bottom curve) and a constant absolute bandwidth contrast sensitivity function (top

curve). Both functions were measured at 100 candela/meter^2. The symbols represent the models fit to the data. As stated above, a 1.5 cycle constant relative bandwidth grating stimulus will only produce robust responses in a few cortical mechanisms. However, a 2.5 degree constant absolute bandwidth stimulus will stimulate many mechanisms. In the Human Performance Model, the increased contrast sensitivity of the constant absolute bandwidth curve is primarily due to probability summation across the difference response of the cortical mechanisms. The HPM equation that controls pooling across mechanisms is provided below.

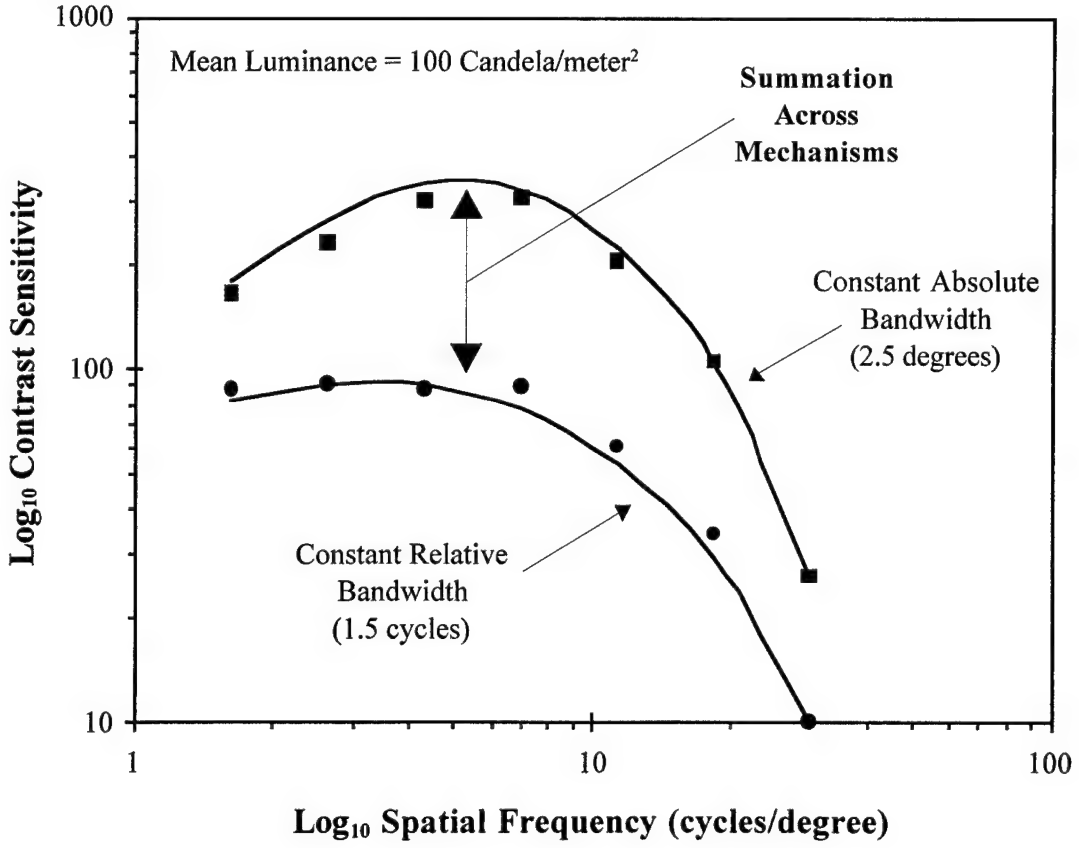

Figure 6. Probability Summation across mechanisms.

3.3.2 System Equation

There are two parameters that affect the degree of summation across mechanisms. The first is N, the number of mechanisms which contribute to the summation process, and the second is Q which determines the efficiency of the summation process. These parameters are shown in the Quick-Wilson function,

$$D = \left[\sum_{i=1}^{N} |Rtest_i - Rbase_i|^Q \right]^{1/Q}$$

which states that the HPM response (D) is the Qth root of the sum of the absolute difference responses of the individual mechanisms to the test and base stimuli, raised to the Qth power.

Psychophysical studies have shown that as the width of a grating stimulus is increased contrast sensitivity first increases and then stabilizes at about 15 cycles of the grating (Robson and Graham, 1984). Because HOP filters have about 1.5 cycles in their spatial support, approximately 10 filters (with optimal frequencies equal to the grating frequency) are required to span the width of this stimulus and 100 filters will be required to fully cover (considering overlap in spatial support) a 15 cycle by 15 cycle grating. Therefore N in the Quick-Wilson equation was set equal to 100.

Examination of the Quick-Wilson function shows that if $Q = 1$ summation is linear. If we hold the difference responses of all mechanism pairs constant and increase Q, then the HPM response decreases. In the limit, ($Q = \infty$) the HPM becomes a peak detector, i.e. the HPM response will be determined exclusively by the maximum difference response. If we define the probability summation efficiency as the HPM response relative to the HPM response when summation is linear, $Q = 1$, then the effect of changing Q on probability summation efficiency for 100 mechanism pairs with identical difference responses is shown in Figure 7.

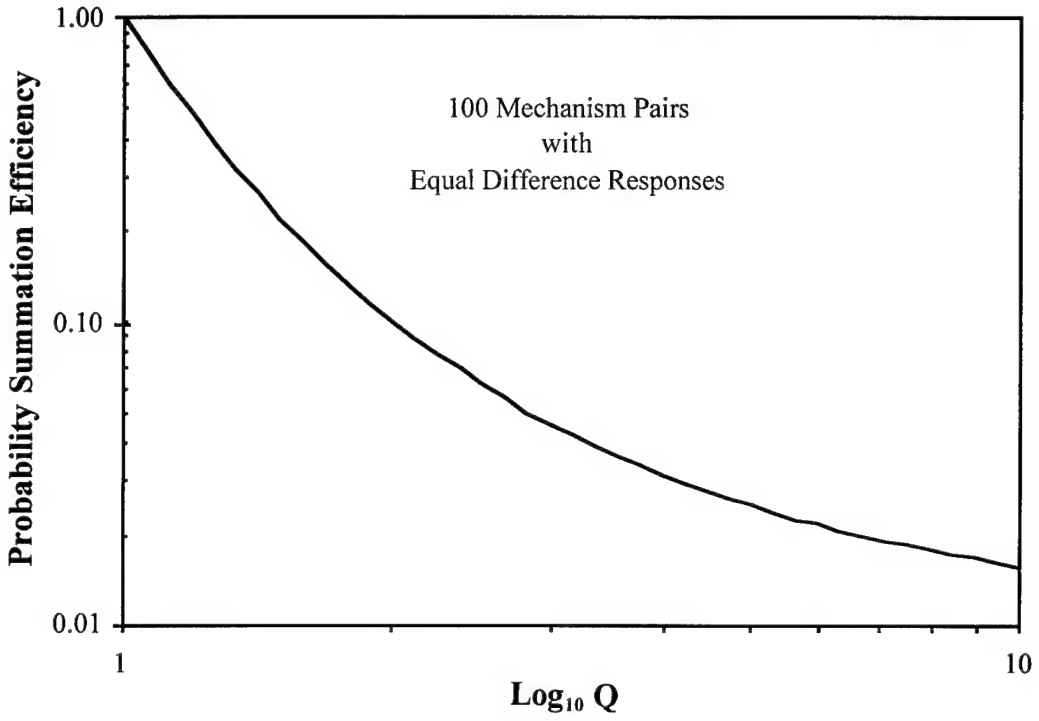

Figure 7. The Effect of Q on Probability Summation Efficiency.

In the model Q changes as a power function of the response of the most sensitive mechanism in the Human Performance Model,

$$Q(R_{\max}) = A_Q + (R_{\max})^{B_Q}$$

where $R_{\max}$ is the value of the maximum responding mechanism (either *Rtest* or *Rbase*) and A_Q and B_Q are parameters whose values are fit by simplex iterative minimization (Press, Flannery, Teukolsky and Vetterling, 1988). In the HPM, Q changes from about 2.5 at contrasts near absolute thresholds to about 10 at high contrasts which is similar to values obtained in psychophysical studies (Wilson 1980, Watson 1987). Evidence that Q changes as a power function of contrast is provided in Wilson (1980).

3.4 Contrast Gain Control

3.4.1 System Equation

Contrast gain control was implemented in the model using the following equation,

$$R_i = \frac{S_i}{k\left(\sum_j w_j s_j\right)^d + 1}$$

where:

- R_i is the response if the i_{th} cortical mechanism,
- S_i is the squared modulus of the HOP transform corresponding to i_{th} cortical mechanism,
- $\sum_j w_j s_j$ is a weighted (w_j) sum of squared moduli, and
- k and d are constant parameters to be fit.

A mechanistic interpretation of the equation is shown below.

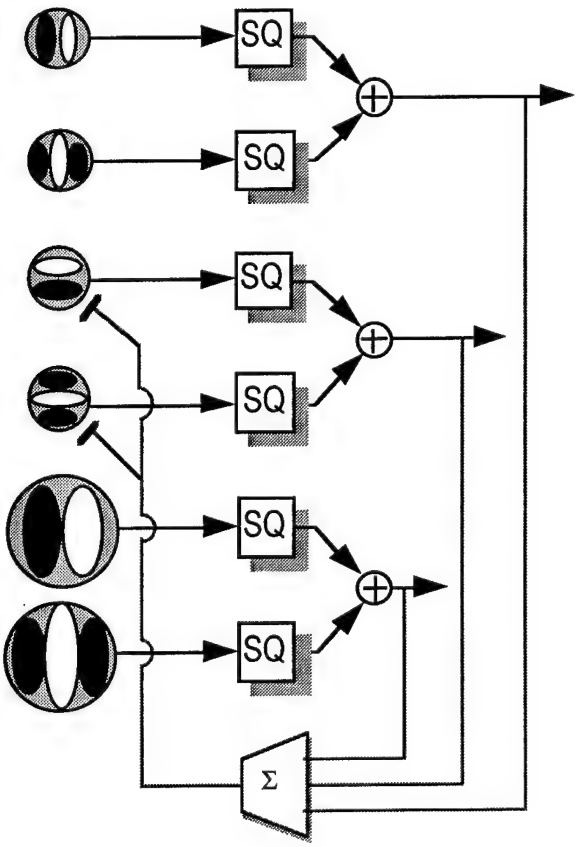

Figure 8. Diagram of Contrast Gain Control.

The cartoon-like receptive-field characterizations on the left hand side of Figure 8 represent the application of individual HOP gabor filters to the image to produce corresponding HOP transform coefficients. The odd and even symmetric coefficients are squared (SQ) and summed to produce a squared modulus. A weighted summation of the squared moduli determines the strength of a feedback signal that divides the HOP coefficients. This model has recently been shown to be consistent with the data obtained from both simple and complex cells in the primary visual cortex (Heeger, 1991).

Figure 9 shows the contrast response function of a cortical mechanism at low contrast (0.0 - 0.2). At very low contrast, where the feedback signal is very small, the denominator of the above equation is approximately 1.0 and the response is approximately equal to the squared modulus. As contrast is increased, the feedback begins to contribute to the denominator and the response begins to compress. The compression is shown more clearly in Figure 10 in which the response is shown over a contrast range of 0.0 - 1.0.

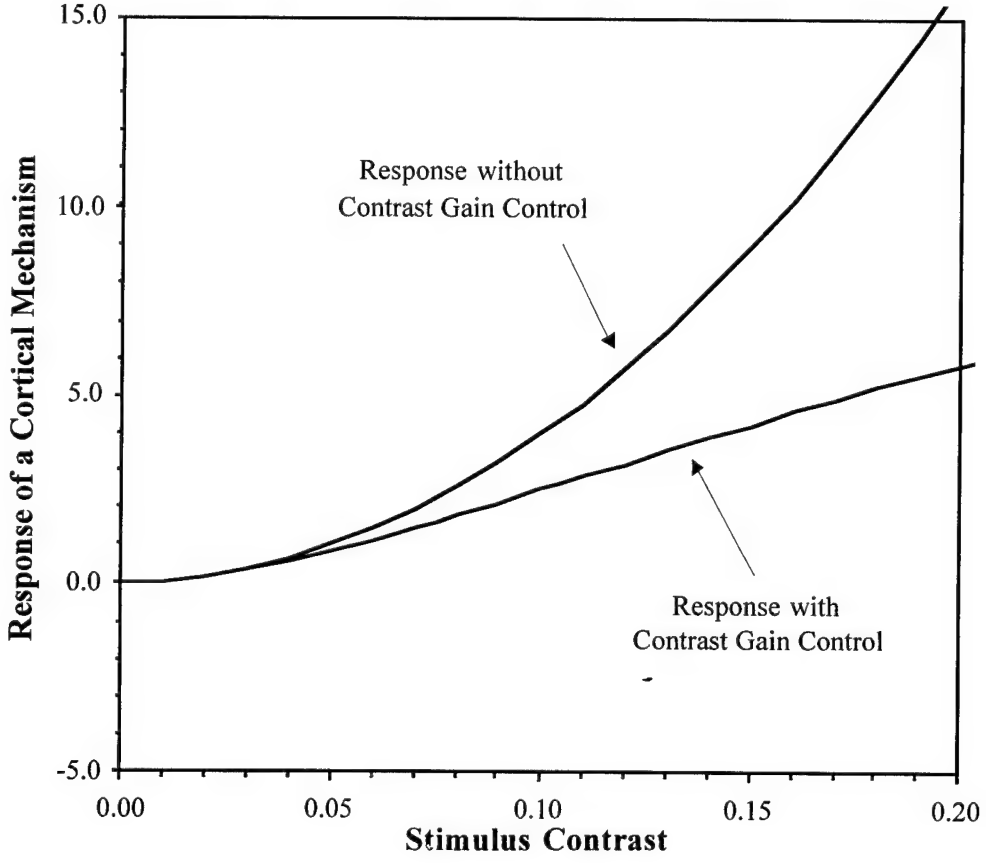

Figure 9. Contrast Response Function of a Cortical Mechanism with and without Contrast Gain Control.

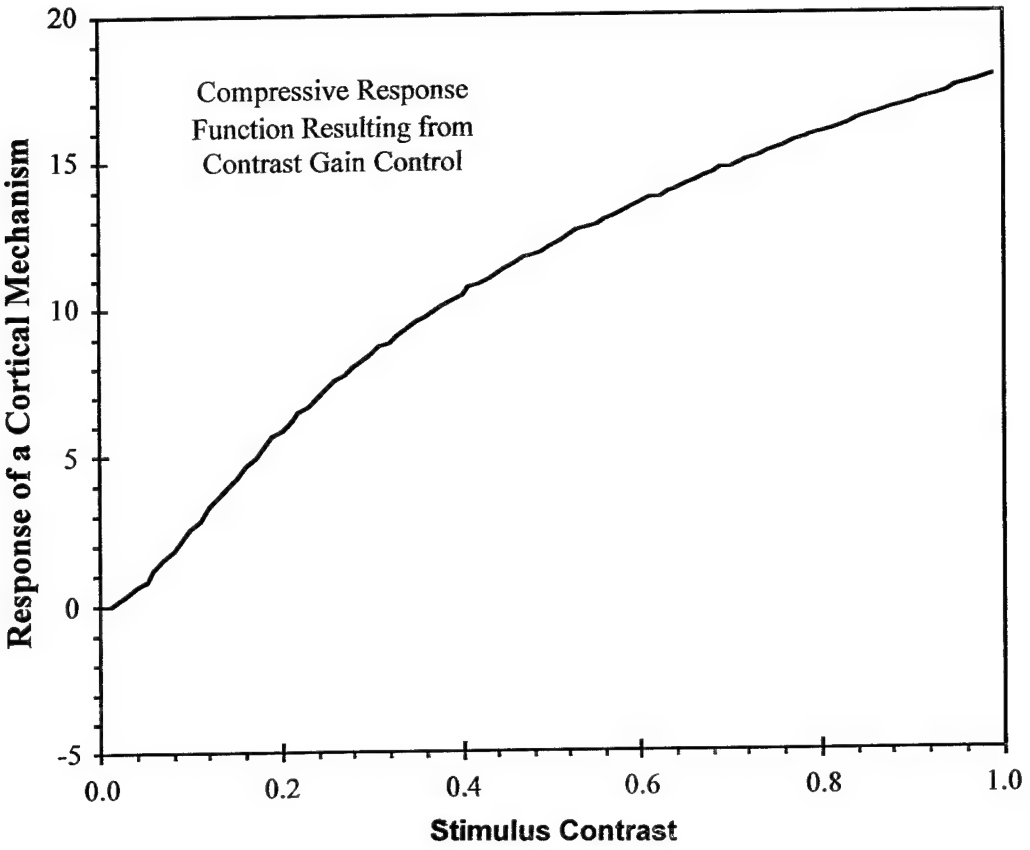

Figure 10. Contrast Response Function of a Cortical Mechanism.

3.4.2 Psychophysical Data

In order to calibrate the contrast response function of the HPM we must compare the model with suprathreshold psychophysical data. Figure 11 shows increment threshold data provided in Legge (1984). In this study the subject was presented with two stimuli. The first stimulus consisted of a sinewave grating of fixed contrast which we will call the background (Rbase). The second stimulus (Rtest) was a sinewave grating that was identical to the first grating except that the contrast was variable. Legge used a two-alternative forced choice technique (discussed above) to determine the contrast difference between the background and test required to produce a 75% correct response (contrast threshold). Legge repeated this procedure using a variety of background contrasts and spatial frequencies.

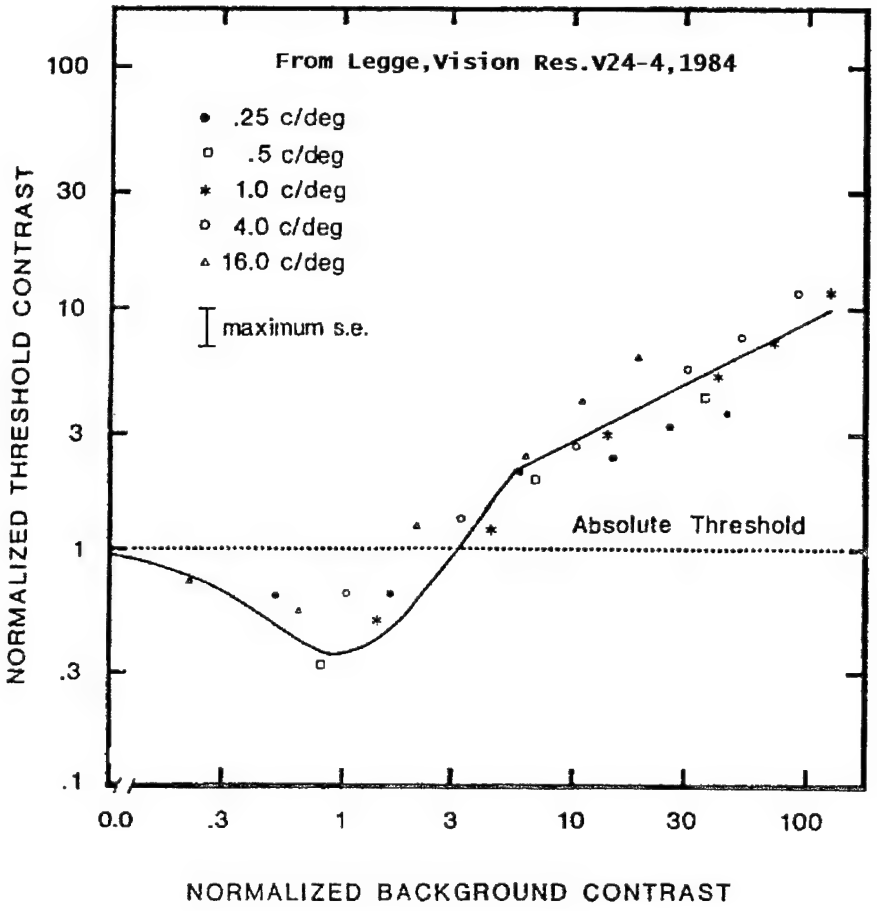

Figure 11. Normalized increment threshold data.

There are three prominent features of this data. First, at low contrasts there is a dip in the data indicating that threshold contrast for discrimination is less than absolute threshold (horizontal dotted line). Second, as the background contrast is increased the threshold contrast begins to rise and cluster near the straight line, which in this figure is a power function with an exponent of 0.5. Finally, the data from all spatial frequencies (when suitably normalized) cluster around a single template given by the solid line in the figure.

The normalization factor used to generate this figure was the absolute threshold of the background stimulus, i.e.,

$$c_{norm}(c) = \frac{c}{T_{abs}}$$

where c is contrast and T_{abs} is the absolute threshold of the background stimulus and c_{norm} is the normalized contrast.

Of course, the normalized threshold contrasts (vertical axis) for the different spatial frequency gratings must equal 1 when background contrast is 0 because we are simply dividing the absolute threshold contrast of the stimulus by itself. More interesting is the finding that when the background contrast is divided by the normalization factor the minimum of the dip in the increment threshold data for all frequencies occurs near a normalized background contrast of 1 and that the threshold contrasts measured at higher background contrasts cluster near the straight line in Figure 11. The straight line in the figure is a plot of the following power function

$$T(c_{norm}) = (c_{norm})^{0.5}.$$

This experiment provides compelling evidence that the *contrast response function* of the visual system is relatively *invariant* as a function of spatial frequency.

This data also provides evidence about the shape of the visual system's contrast response function. If the contrast response function of the HPM was linear, then increment thresholds would be independent of background contrast, i.e. the data would fall on the dotted line labeled absolute threshold. However the data show that threshold contrasts decrease at low contrasts and increase at higher contrast. The data is therefore consistent with the model's contrast response function shown above which has an accelerating nonlinearity at low contrasts followed by a compressive nonlinearity at high contrasts (Figures 9 and 10).

3.4.3 Calibration Results

Legge's finding has been replicated and extended by several studies (Bradley and Ohzawa, 1986; Ross and Speed, 1991). All of the studies show that if increment threshold data are normalized by absolute thresholds then the data cluster near a canonical template. However the intercept and exponent of the power function describing threshold contrasts at high background contrast is clearly different across the various studies. We fit the Human Performance Model at high backgrounds contrasts with a power function having an intercept of 0.5 and an exponent 0.7,

$$T(c_{norm}) = 0.5(c_{norm})^{0.7}$$

which constitute the most representative values across the various studies.

The results provided by this calibration are shown in Figure 12 for stimulus spatial frequencies of 1, 4, and 16 cycles/degree. These data are plotted as Normalized Threshold Contrast values to facilitate comparison with Legge's data in Figure 11.

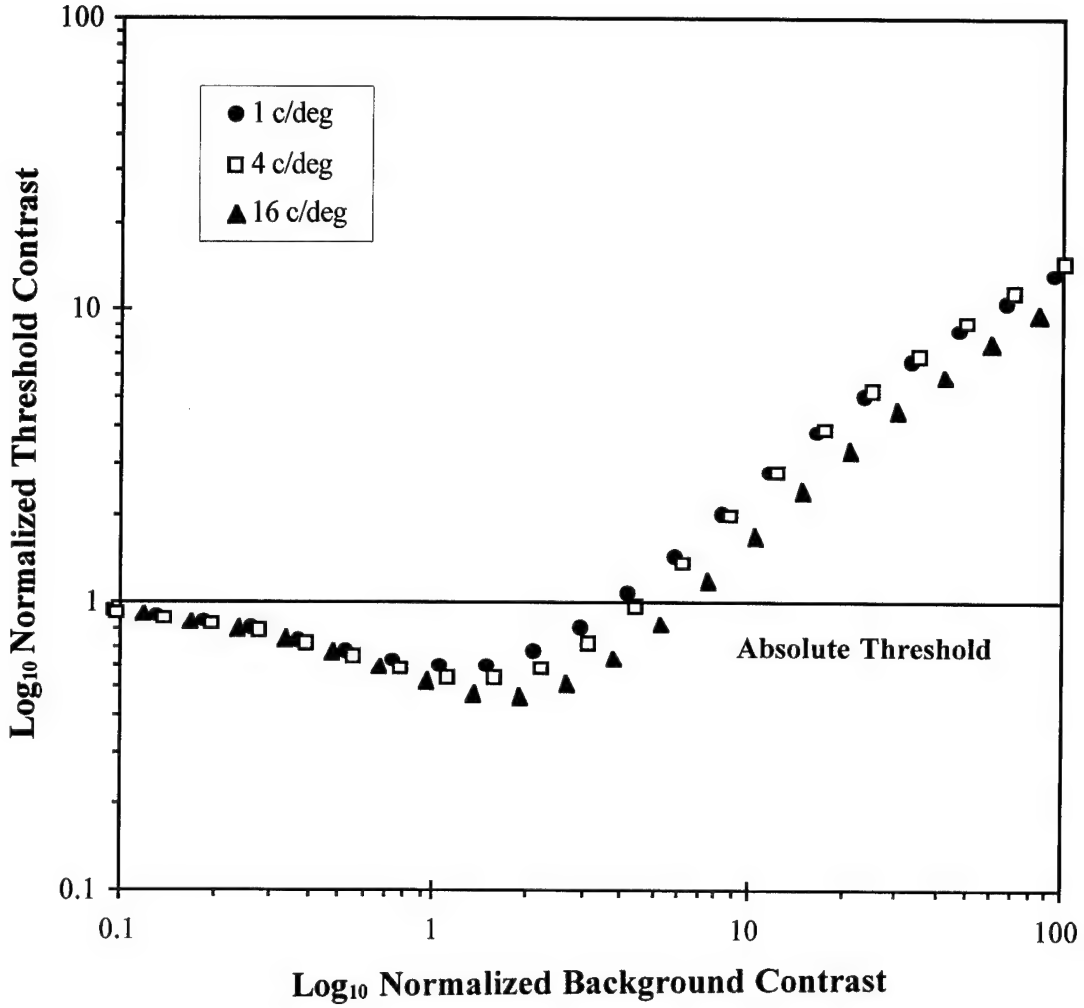

Figure 12. Normalized increment thresholds of model.

4. APPLICATION OF THE HUMAN PERFORMANCE MODEL

The HPM has been implemented as a set of four modules that can be linked into the user's application. A demonstration program included on a distribution diskette serves to illustrate the use of these functions in a complete application that reads in a pair of user-specified images and prints out an estimated human sensitivity value. An abbreviated version of the demonstration program appears in Listing 1 below. The functions InitModelParameters, ApplyLgnFilter, ApplyCortexTransform, and ComputeSensitivity make up the complete interface to the HPM library (see steps 3, 4, 5 and 6 in Listing 1). The main module of the demonstration program also calls several other functions which are defined in the complete demonstration software source listings. These functions serve to "read" the pair of images and their associated parameter file.

```
/*
        DEMO - Abreviated main program.
                Usage: demo image1.tif image2.tif
*/
#include <stdio.h>
#include "../hpmlib/hpm.h"
#include "demo.h"
main(int argc, char *argv[])
        {
        IMAGEPARAMETER ImageParam;
        LGNPARAMETER LgnParam;
        CORTEXPARAMETER CortexParam;
        DISCRIMPARAMETER DiscrimParam;
        ROI RegionOfInterest;
        MULTICHROME *pImage1;
        MULTICHROME *pImage2;
        MULTICHROME *pLgn1;
        MULTICHROME *pLgn2;
        MULTICHROME *pCortex1;
        MULTICHROME *pCortex2;
        float fMeanLum1;
        float fMeanLum2;
        float fLuminance;
        float fSensitivity;
        //
        // (1) READ IMAGE PARAMETERS FROM INITIALIZATION FILE
        //
        ReadImageParameters("image.ini", &ImageParam);
        //
        // (2) READ AND RESCALE IMAGE PAIR & COMPUTE MEAN LUMINANCES
        //
        pImage1 = ReadImage(argv[1], &ImageParam, &fMeanLum1);
        pImage2 = ReadImage(argv[2], &ImageParam, &fMeanLum2);
        //
        // (3) INITIALIZE PARAMETERS USING SPECIFIED BACKGROUND LUMINANCE
        //
        fLuminance = max(fMeanLum1, fMeanLum2);
        InitModelParameters(&LgnParam, &CortexParam, &DiscrimParam, fLuminance);
        //
        // (4) APPLY LGN FILTER TO RECT IMAGES TO OBTAIN FILTERED HEX IMAGES
        //
        pLgn1 = ApplyLgnFilter(pImage1, &ImageParam, &LgnParam);
        pLgn2 = ApplyLgnFilter(pImage2, &ImageParam, &LgnParam);
        //
        // (5) APPLY CORTEX TRANSFORM TO PAIR OF FILTERED HEX IMAGES
        //
        GetROIForReferenceImage("image.ini", &RegionOfInterest);
        pCortex1 = ApplyCortexTransform(pLgn1, &RegionOfInterest, &CortexParam);
        GetROIForTestImage("image.ini", &RegionOfInterest);
        pCortex2 = ApplyCortexTransform(pLgn2, &RegionOfInterest, &CortexParam);
        //
        // (6) COMPUTE DISCRIMINABILITY OF PAIR OF CORTEX REPRESENTATIONS
        //
        fSensitivity = ComputeSensitivity(pCortex1, pCortex2, &DiscrimParam);
        printf("Discrimination sensitivity = %f\n", fSensitivity);
        }
```

The demonstration program illustrated above represents the most basic application of the HPM to implement a system that predicts human performance in a *discrimination* task. The demonstration program can also predict human performance in a simple *detection* task (i.e., target on uniform background) if one specifies one of the two input images as a uniform luminance field.

The Human Performance Model has been designed to provide the basis for the development of more sophisticated applications. In particular, the HPM has been designed to facilitate the construction of diverse systems that act as surrogate human observers. A surrogate human observer is here defined as any automated system used to predict human visual psychometric functions without having to conduct psychophysical experiments with real human subjects.

For example, there are many situations where one would like to know how human discrimination sensitivity varies as a function of an independent variable. In particular, one might be given target and decoy infrared (IR) images collected at regular intervals throughout the day. Taking these image pairs as input, a simple application could use the HPM to produce a plot of predicted human target vs. decoy discrimination sensitivity as a function of time-of-day. Note, that the target and decoy objects should be presented against equal backgrounds, be depicted from equal viewpoints, and hence differences in their images should reflect only intrinsic differences in shape and thermodynamic properties.

There are also many situations where one desires the accurate prediction of human visual performance in more complicated tasks, such as detecting a target on a cluttered background, target recognition, and target identification. Fortunately, human visual performance tasks such as these can often be formulated in terms of paired image discriminations. After so reformulating the problem, one can then proceed to develop an application that uses the HPM to predict human performance in these more complicated tasks.

5. REFERENCES

Barten, P. G. (1990) Evaluation of subjective image quality with the square integral method. *Journal of the Optical Society of America-A* 7, 2024-2031.

Carlson, C. R. (1982) Sine-wave threshold contrast sensitivity function: dependence on display size. *RCA Review 43*, 675-683.

Heeger, D. J. (1991) Normalization of cell responses in cat striate cortex. *Visual Neuroscience* 9, 181-197.

Irvin, G.E., Casagrande, V.A., Norton, T.T. (1993) Center-Surround Relationships of Magnocellular, Parvocellular and Koniocellular Relay Cells in Primate Lateral Geniculate Nucleus. Visual Neuroscience, 10, 363-373.

Irvin, G.E., Norton, T.T. & Casagrande, V.A. (1986) Receptive-field Properties Derived from Spatial Contrast Sensitivity Measurements of Primate LGN Cells. *Invest. Ophthal. and Vis. Sci. Suppl.*, 27.

Johnson, J. Analysis of Image Forming Systems. Image Intensification Symposium, Fort Belvoir, VA October 6-7, 1958.

Kelly, D. H. (1972) Adaptation effects on spatio-temporal sine-wave thresholds. *Vision Research* 12, 89- 97.

Bradley, A. and Ohzawa, I. (1986). A comparison of contrast detection and discrimination. *Vision Research* 26, 991-997.

Legge, G. E. (1984) Binocular contrast summation-II. Quadratic summation. *Vision Research* 24, 385-394.

Press W. H, Flannery B. P., Teukolsky S.A., Vetterling W. T. (1988) *Numerical recipes in C,* Cambridge University Press, Cambridge, MA.

Quick R. F. (1974) A vector-magnitude model for contrast detection. *Kybernetic* 16, 65-67.

Robson, J. G. and Graham N. (1981) Probability summation and regional variation in contrast sensitivity across the visual field. *Vision Research* 21, 409-424.

Rodieck, R. W. (1965) Quantitative analyses of cat retinal ganglion cell response to visual stimuli. *Vision Research* 5 583-601.

Ross, J. and Speed, H. D. (1991) Contrast adaptation and contrast masking in human vision. *Proceedings of the Royal Society of London, B*, 246,61-69.

van Meeterin, A. (1973) Visual aspects of image intensification. *Ph.D. Dissertation* (University of Utrecht, Utercht, The Netherlands).

Watson A. B. (1987) Efficiency of an image code based on human vision. *Journal of the Optical Society of America-A 4*, 2401-2417.

Watson A. B. (1990) Perceptual-components architecture for digital video. Journal of the Optical Society of America-A 7, 1943-1968.

Watson A. B. and Ahumada, A. J. Jr. (1987) On orthogonal oriented quadrature hexagonal image pyramid. *NASA Technical Memo 100054* (National Aeronautics and Space Administration, Washington, DC).

Wilson H. R. (1980) A transducer function for threshold and suprathreshold human vision. *Biological Cybernetics* 38, 171-178.